

# Precision laser development for interferometric space missions NGO, SGO, and GRACE Follow-On

**K Numata<sup>1,2</sup>, J Camp<sup>2</sup>**

<sup>1</sup>University of Maryland, Department of Astronomy/CRESST, College Park, Maryland 20741 USA

<sup>2</sup>NASA Goddard Space Flight Center, Greenbelt, Maryland 20771, USA  
E-mail: kenji.numata@nasa.gov

**Abstract.** Optical fiber and semiconductor laser technologies have evolved dramatically over the last decade due to the increased demands from optical communications. We are developing a laser (master oscillator) and optical amplifier based on those technologies for interferometric space missions, including the gravitational-wave missions NGO/SGO (formerly LISA) and the climate monitoring mission GRACE Follow-On, by fully utilizing the matured wave-guided optics technologies. In space, where simpler and more reliable system is preferred, the wave-guided components are advantageous over bulk, crystal-based, free-space laser, such as NPRO (Non-planar Ring Oscillator) and bulk-crystal amplifier.

## 1. Introduction

Three space missions are now being planned that will use precision interferometry to achieve very high displacement sensitivity. In Europe, the gravitational wave mission NGO, aiming for launch in 2022, will use laser interferometry to monitor the motion of freely falling test masses in spacecraft separated by  $\sim 10^9$  m. In the US, a number of concepts are under study for the SGO mission, including both laser and atom interferometry, requiring the use of low-noise lasers to enable the measurement of gravitational waves. SGO may launch by the end of the next decade. (While the designs of NGO and SGO are under discussion, they are both closely related to LISA [1], the former joint US-European collaboration, and to be conservative we refer to the more stringent LISA laser requirements in this article.) Finally, the GRACE Follow-On mission [2], planned for launch in 2016, will use laser interferometry between spacecraft separated by  $\sim 200$  km to monitor the time-varying gravity fields of the earth.

Laser technology for the telecom industry has undergone dramatic advances in the past decade, replacing lasers and optical amplifiers based on bulk optics with technology including fiber laser/amplifier, waveguide devices, and semiconductor lasers. These components naturally fit into the precision laser systems needed for the interferometric missions, because of their high mechanical robustness, high reliability, compact form factor, and high wall-plug efficiency. We are pursuing all-fiber/waveguide space laser solution based on the MOFA (master oscillator fiber amplifier) configuration, namely, a waveguide-based oscillator followed by a pre-amplifier and a power amplifier. We are developing both 1.06  $\mu$ m and 1.55  $\mu$ m systems for NGO, SGO, GRACE Follow-On, and potentially other lidar missions.

## 2. Master oscillator

We have developed fiber ring laser and fiber DBR laser, both of which are based on wide-bandwidth fiber Bragg grating (FBG), Fabry-Perot FBG, and Yb-doped gain fiber for 1.06  $\mu\text{m}$  [3]. Although these lasers have comparable performance to the non-planar ring oscillator (NPRO) at low ( $<10$  kHz) frequency, they have larger relaxation oscillation peak around 1 MHz, which could affect the heterodyne interferometry typically operated near this frequency. These fiber lasers also tend to have a large number of optical components, resulting in questions about their reliability. In this paper, we introduce the planar-waveguide external-cavity diode laser (PW-ECL), which we have identified to be a simple and robust design and thus promising for the space applications. It also has the proven reliability by the Telcordia GR-468 standard and the best low-frequency performance among the lasers we have tested.

### 2.1. PW-ECL design

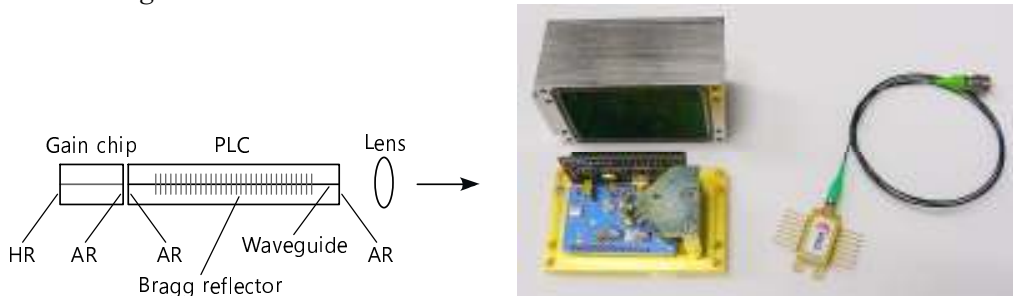


Fig.1. (Left) schematic of the PW-ECL. HR: high-reflective coating, AR: anti-reflective coating, PLC: planar lightwave circuit. (Right) Photo of core optics of NPRO and the PW-ECL package. In the PW-ECL butterfly package, the output is PM fiber-coupled after the lens and an optical isolator.

The PW-ECL evaluated here is commercial product (named PLANEX), built by Redfern Integrated Optics (RIO). Figure 1 (left) shows schematic of the cavity of the PW-ECL. The laser cavity is formed by two reflectors: a high-reflective (HR) coated facet on an InP multiple quantum well gain chip, and an anti-reflection (AR) coated waveguide grating formed in a silica-on-silicon planar lightwave circuit (PLC). All components are integrated into a standard 14-pin butterfly package on top of a thermoelectric cooler. As shown in Fig.1 (right), the package is much more compact than that of NPRO, in which a strong magnet fundamentally limits the size. The narrow reflection peak of the Bragg reflector in the PLC enables stable, low-noise, single-mode lasing at a selected wavelength within the telecom C-band (1528~1565 nm). Typical output power is  $\sim 15$  mW.

### 2.2. PW-ECL noise performance

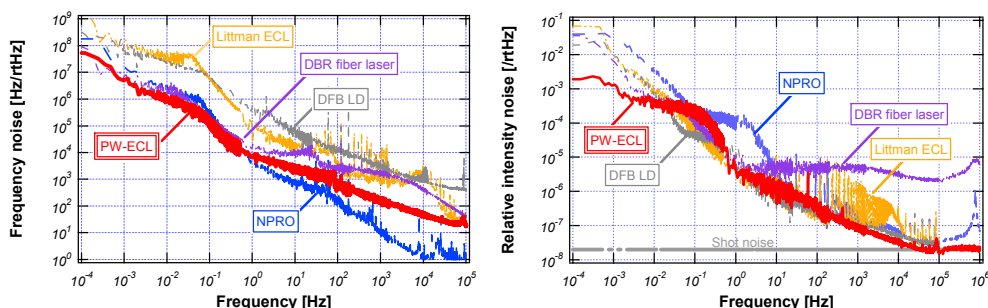


Fig.2. Free-running frequency (left) and relative intensity (right) noise spectra of various single-frequency lasers. PW-ECL: PLANEX from Redfern Integrated Optics (1542 nm), NPRO: Model 125

from Lightwave Electronics (1064 nm), DBR fiber laser: ROCK from NP Photonics (1542 nm), Littman ECL: Lion from Sacher Lasertechnik (1064 nm), DFB-LD: FRL15DCWD from Fitel (1578 nm).

As shown in Fig. 2, the PW-ECL has a sufficiently low level of frequency and intensity noise to be suitable for precision measurement applications. The noise level was comparable or better than the NPRO and fiber laser between 0.1 mHz to 100 kHz. Controllability of the PW-ECL was also demonstrated by stabilizing its frequency to hyperfine line of acetylene at  $10^{-13}$  level of Allan deviation [4], by phase locking between two PW-ECLs, and by Pound-Drever-Hall frequency locking to high finesse ( $\sim 20,000$ ) optical cavity.

### 2.3. Space qualification tests

We have performed various tests on the PW-ECL to investigate its suitability for a space qualification program. All performance and reliability testing done to date has indicated that the PW-ECL is robust for spaceflight. Some of the test results are introduced below.

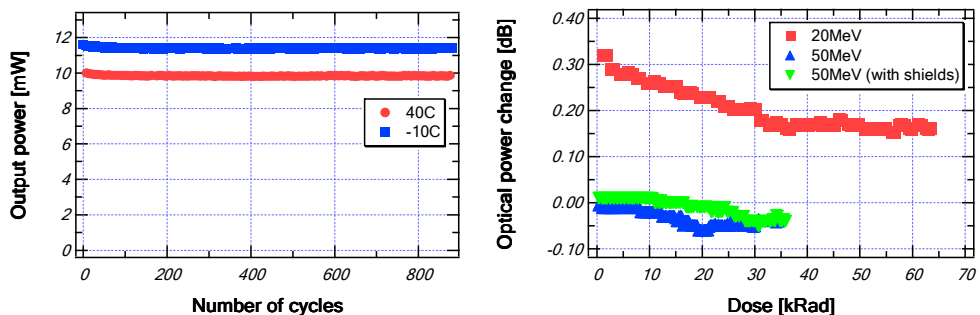


Fig.3. (Left) Vacuum thermal cycling test result of PW-ECL. Output powers of the two temperature extremes are plotted. (Right) Proton radiation test result of PW-ECL.

- Active vacuum thermal cycling was carried out between  $-10$  to  $+40^\circ\text{C}$ , over 1000 cycles. The power levels at the temperature extremes had differences in the range of 0.5 to 1.8 mW at the nominal 10 mW output level (Fig.3, (left)). This was explained as due to a slight temperature difference between the gain chip and PLC at the two temperature extremes. All module tested show very little or no degradation. Additional tests over a temperature cycling range of  $-25$  to  $+80^\circ\text{C}$  showed similar steady performance of the PW-ECL.
- Hermeticity testing commenced with a  $100^\circ\text{C}$  bake for 16 hours, followed by lid sealing with a nitrogen-helium fill gas, fine-leak testing and thermal cycling ( $-43$  to  $+93^\circ\text{C}$ , 20 cycles). The final fine leak, gross leak and residual gas analysis showed that the modules remained hermetic, which greatly reduces possibility of material degradation over long time.
- The PW-ECL module was subjected to a total dose of 200 krad of 1 MeV gamma rays from a  $\text{Co}^{60}$  source behind an aluminum plate with 2.5-mm thickness. Small changes were noted in the wavelengths ( $\approx +10$  pm) and the output power ( $\approx -0.30$  dB), both in situ and 2 days after the termination of the irradiation. Under proton beam at 20 MeV and 50 MeV and total dose of few kRad, the maximum change in wavelengths was  $\approx +50$  pm. There was recovery several days after that stabilized at  $\approx +25$  pm. The maximum change in output powers was  $\approx -0.15$  dB (Fig.3, (right)). There was no mode hop during those irradiations and no significant changes in the phase noise performance after the irradiation. These tests were performed at a highly accelerated rate to fluence values on the order of 100 times those expected over 5 years on the orbit.

## 2.4. Future activities

Future activities planned for the PW-ECL for use in space include: 1) Development of 1064-nm version by using different gain chip material and PLC design while keeping other mechanical design, 2) Introduction of small phase modulation section within the gain chip in order to expand the frequency tuning bandwidth from  $\sim 10$  kHz to  $\sim 10$  MHz, 3) Irradiation testing with low-energy proton, 4) Frequency locking to optical cavity to achieve thermal noise level frequency noise performance (at Univ. of Texas Brownsville), and 5) 1/f frequency noise level reduction by using different gain-chip design.

## 3. Pre-amplifier

The  $\sim 10$  mW output of PW-ECL itself may be sufficient for the GRACE-FO mission, and as a seed laser for the power amplifier in the LISA mission where  $\sim 2$  W level of power is required. However, in order to have power margin and to be flexible for changing mission requirements, we are developing fiber pre-amplifiers with output power of  $\sim 200$  mW both at  $1.06\ \mu\text{m}$  and at  $1.55\ \mu\text{m}$ . Both are common wavelengths for laser-communication and lidar applications.

### 3.1. Design

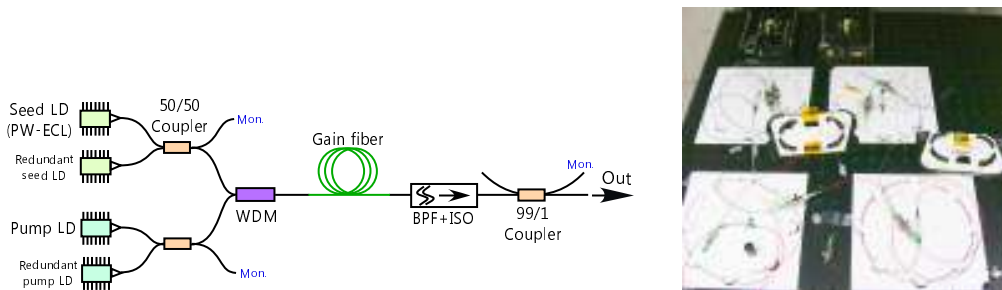


Fig.4. (Left) Conceptual design of seed laser + pre-amplifier system. WDM: wavelength-division multiplexing coupler, BPF: band-pass filter, ISO: optical isolator. (Right) Photograph of preamplifier system under test.

Figure 4 (*left*) shows the design of the seed laser and the pre-amplifier system. The laser unit will house two seed lasers (PW-ECLs) and two pump laser diodes for redundancy, as well as their control circuits. All fiber components are single-mode, polarization-maintaining. The gain fiber is  $\sim 2$ -m long and core-pumped. The pump LD is at  $\sim 976$  nm, which is more reliable than the 808 nm LD for the Nd:YAG lasers in the space.

### 3.2. Preamplifier noise performance

Using 1542-nm PW-ECL seed and Er-doped gain fiber, we built test pre-amplifier (without redundant LDs). For 1064-nm system, we are using Yb-doped gain fiber and seed NPRO, which will be eventually replaced by 1064 nm PW-ECL, currently under development by RIO. Figure 5 shows noise performance of the 1542-nm preamplifier, where 9-mW PW-ECL input is amplified to 180 mW. The preamplifier adds negligible frequency noise (Fig.5 (*left*)). The preamplifier adds intensity noise especially at low frequency (Fig.5 (*right*)). This excess noise can be suppressed by controlling the pump power.

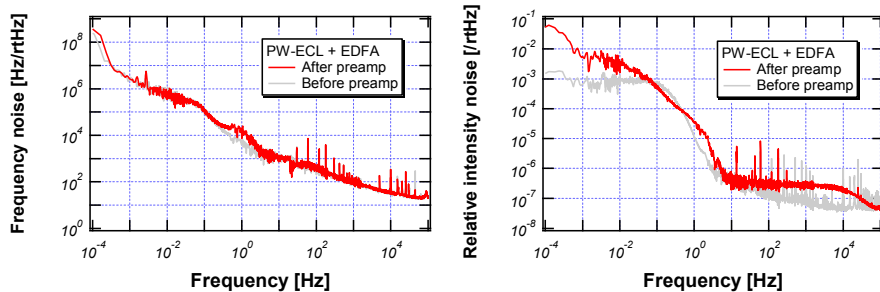


Fig.5. (Left) Frequency noise and (Right) relative intensity noise before and after the Er-doped preamplifier seeded by 1542-nm PW-ECL.

### 3.3. Space qualification tests

The fiber-based preamplifier power level is low and thus the system components are not expected to present risk for flight; however, radiation hardness is an important remaining factor in the qualification of pre-amplifier components. We have performed gamma irradiation tests on 1.06- $\mu\text{m}$  Yb amplifier components, which are less matured than the 1.55- $\mu\text{m}$  components. The tested components include Yb-doped gain fiber, optical band-pass filter with isolator, and coupler.

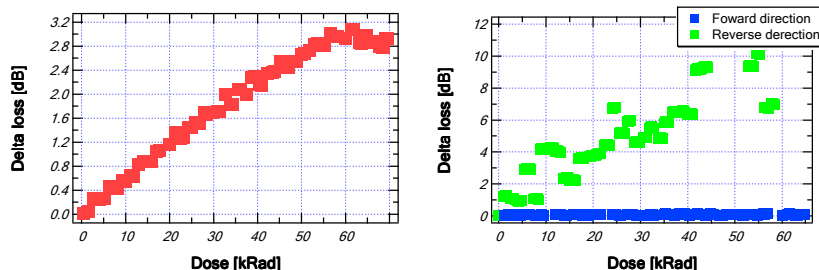


Fig.6. Gamma irradiation testing results of preamplifier components. Vertical axes represent change in the insertion loss. (Left) Yb-doped gain fiber (5-m length). Irradiation was terminated at 60 kRad. (Right) 1.064- $\mu\text{m}$  band-pass filter isolator.

Figure 6 shows results example. Yb-doped gain fiber (1200-dB/m small signal absorption at 976 nm) showed typical increase in loss of  $\sim 0.6$  dB/m with 60 kRad dose (Fig.6, (left)). This value is typical for doped fibers under the high dose rate. Such damage will be much lower at lower dose rate expected during the mission and will be mitigated by the photo-annealing effect. The filter-isolator showed  $\sim 0.15$  dB and  $\sim 10$  dB increase in loss for the forward and reverse directions, respectively (Fig.6, (right)). The performance and functionality of the isolator were not affected by the irradiation.

### 3.4. Current activities

We are identifying components to be used in the preamplifier package and evaluating test preamplifiers. We are also designing space-qualifiable low-noise current driver based on the design shown in [5]. The goal is to have a compact oscillator-preamplifier module with integrated electronics at a total electrical power consumption of 10 W.

#### 4. Power amplifier

We are working with Lucent Government Solutions to develop Yb fiber amplifier for the NGO/SGO missions. The wavelength is 1.06  $\mu\text{m}$ .

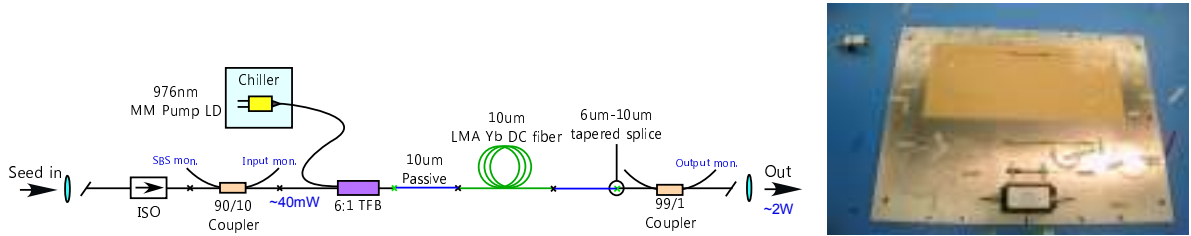


Fig.7. (Left) fiber amplifier configuration. ISO: optical isolator, TFB: tapered fiber bundle. (Right) photograph of the amplifier breadboard.

##### 4.1. Design

After various trade studies and simulations, the fiber amplifier shown in Fig. 7 was constructed. A 976-nm pump LD was selected over 915-nm, since it was expected to have better performance (efficiency, noise figure, and temperature insensitivity) in our simulation. A 10- $\mu\text{m}$  core, double-clad (DC), large mode area (LMA) fiber was selected as a gain media to elevate the SBS (stimulated Brillouin scattering) threshold. The length of the gain fiber is about 5 m. It is forward, clad-pumped through a tapered fiber bundle (TFB, 6:1 pump combiner). The forward-pumping design minimizes potential sources of feedback (e.g. from the TFB). Such feedback could result in lasing and in catastrophic damage, which we found to occur in our prototype backward-pumped amplifiers. The simple single-stage amplifier design gives  $\sim 2$  W output ( $\sim 6$  W maximum) with 40-mW seed input and 5-A pump current on the fiber-coupled 10-W pump LD. Redundant pump LDs can be attached to unused ports of the TFB. The TFB was identified as the most risky component within the amplifier, and was pre-screened by a thermal imager and re-packaged using suitable compounds for higher reliability in space. This design was characterized for optical efficiency ( $\sim 68\%$ ), polarization extinction ratio (PER, 17~32 dB, with 20 dB typical), and noise figure of 5 dB.

##### 4.2. Amplifier performance

We are evaluating frequency (phase) noise performance of the power amplifier and the results are shown in Fig. 8. In these figures, commercial NPRO was used as a seed source.

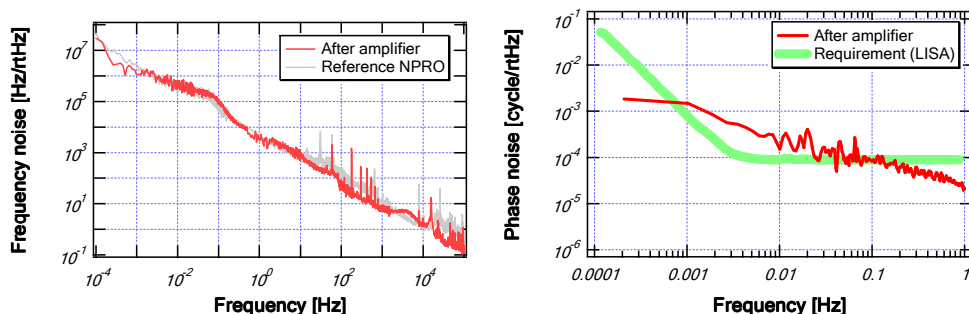


Fig.8. (Left) Free-running frequency noise of the NPRO and the amplifier output at 2 W. (Right) Differential phase noise of the amplifier at 2 W.

The power amplifier adds negligible frequency noise to the carrier light of the seed as depicted in Fig. 8 (*left*). Any frequency noise added by the amplifier would be suppressed by the frequency stabilization control loop, whose light is taken after the amplifier. The differential phase noise (phase noise between the carrier and the clock transfer sideband at 2 GHz) [6] is not suppressed by the control loop and has to be kept low. As shown in Fig. 8 (*right*), the noise level is factor  $\sim 4$  higher than the LISA requirement level. The excess differential phase noise had some correlations to temperature variations (which are not stabilized in our setup) and to the increase in the backscattered power (which indicates the existence of SBS). Our goal is to improve this performance by implementing a stable temperature (which will be present in the spacecraft) and also by modifying the amplifier optics. We have confirmed that the possible SBS component is not affected by the seed laser's linewidth by using an iodine-stabilized NPRO as seed.

The intensity noise of the amplifier was also measured and stabilized. The bandwidth of the intensity control servo was 10 kHz. Figure 9 (*left*) shows the relative intensity noise (RIN) of the amplifier at 2 W output at low frequency. The stabilized level is below the LISA requirement above 1 mHz. We think the excess noise below 1 mHz is not inherent to the amplifier, but due to the temperature variation in the stabilization system. At the higher frequency region (Fig. 9, (*right*)), the RIN is at the shot noise level of  $\sim 1.5$ -mW detected power above  $\sim 5$  MHz with and without the stabilization, as in the seed NPRO only. This indicates shot-noise-limited heterodyne interferometry is possible with the amplifier at this detection power level and with a proper choice of the RF heterodyne frequency.

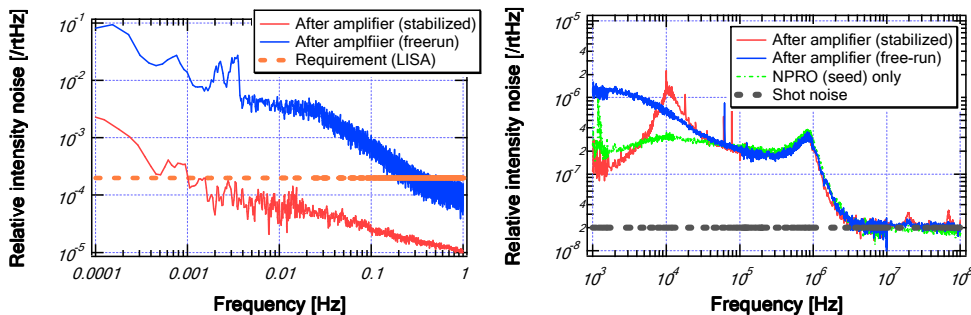


Fig.9. (*Left*) Free-running and stabilized RIN of the amplifier output at 2 W at low frequency. (*Right*) amplifier RIN at high frequency together with seed NPRO's RIN. The stabilized RIN was measured with out-of-loop photo-detector and the band-pass filter.

#### 4.3. Space qualification tests

Vacuum thermal cycling test of the amplifier was conducted by splicing the amplifier breadboard into a thermally controlled vacuum chamber. The temperature of the breadboard was set using temperature-controlled fluid circulated through the base-plate into the vacuum chamber.

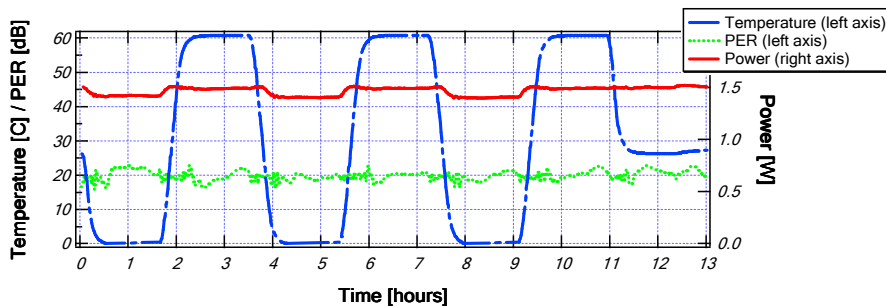


Fig.10. Vacuum thermal cycling result of the power amplifier.

The amplifier showed negligible performance change after 100 hours of vacuum thermal cycling between 0 °C and 60 °C. As an example, Fig. 10 shows data collected during the temperature cycles, including power, PER, and the baseplate temperature.

#### 4.4. Current activities

We are evaluating radiation hardness of a set of gain fibers, including the one used in the prototype amplifier and two other commercial brands. We are further investigating the noise issues, especially its relationship to the SBS (threshold), by adopting slightly different amplifier configurations. The 5-m gain fiber, which generates 6 W maximum, is too long for the NGO/SGO missions that require ~1-W level output. Reducing the lengths of the gain and delivery fibers should improve the noise performance through increased SBS threshold. Selection of an output isolator, a filter to cut out amplified spontaneous emission, and a high-power fiber collimator are also underway.

### 5. Summary

We presented our efforts at the NASA Goddard Space Flight Center on precision laser systems for the interferometric missions NGO, SGO, and GRACE Follow-On. Our approach is based on fibers and waveguides, adapting the matured wave-guided optics technologies of the telecom industry. The fiber approach has numbers of advantages over traditional bulk optics, and will be used as possible in space laser missions in the future. We are characterizing the laser and the amplifier both at the component level and at the system level. We will continue to pursue the development of low-noise space laser systems, bringing in the latest technical advances.

### Acknowledgement

The authors would like to thank Alfonso Piccirilli, Robert Ahrens, Anthony Fields, Gregory Johnson, Leslie Reith, and Gunther Schwarz at Lucent Government Solutions for their technical support on this project. The authors also thank Lew Stolpner and Mazin Alalus at Redfern Integrated Optics for their development work on the PW-ECL.

### References

[1] P. Bender, K. Danzmann, and the LISA Study Team, "Laser interferometer space antenna for the detection of gravitational waves, pre-Phase A report," Tech. Rep. MPQ233, Max-Planck-Institut für Quantenoptik, Garching (1998). 2nd ed.

- [2] M. Stephens, et al., “Demonstration of an Interferometric Laser Ranging System for a Follow-On Gravity Mission to GRACE,” in Proceedings of IEEE International Conference on Geoscience and Remote Sensing Symposium, (IEEE, 2006), pp. 1115~1118.
- [3] K. Numata, J. Chen, and J. Camp, *J. Phys.: Conf. Ser.*, **228** (2010) 012043.
- [4] K. Numata, J. Camp, M. A. Krainak, and L. Stolpner, *Optics Express*, **18** (2010) 22781.
- [5] C. J. Erickson, M. V. Zijll, G. Doermann, and D. S. Durfee, *Rev. Sci. Instrum.* **79** (2008) 073107.
- [6] M. Tröbs, S. Barke, Th. Theeg, D. Kracht, G. Heinzel, and K. Danzmann, *Optics Letters*, **35** (2010) 435.